Study of Spray Cooling Control to Maintain Metallurgical Length During Speed Drop in Steel Continuous Casting

Metallurgical length control is important for operations such as soft reduction. This work explores the small potential to control deviations in metallurgical length during casting speed changes. By dropping spray water flowrates from their greatest to smallest levels, results show that a speed drop of 0.2 m/minute can be accommodated in a 221-mm-thick slab caster while maintaining constant metallurgical length during steady casting. Under transient conditions, however, there is always some deviation.



Authors

Zhelin Chen (top row, left)
graduate research assistant, University of Illinois at Urbana-Champaign, Urbana, Ill., USA
zchen61@illinois.edu

Joseph Bentsman (top row, right)
professor of mechanical engineering, University of Illinois at Urbana-Champaign, Urbana, Ill., USA
jbentsma@illinois.edu

Brian G. Thomas (bottom row)
professor of mechanical engineering, Colorado School of Mines, Golden, Colo., USA
bgthomas@mines.edu

Akitoshi Matsui
senior research manager, Steelmaking Research Department, JFE Steel Corp. Steel Research Lab, Hiroshima, Japan
a-matsui@jfe-steel.co.jp

In the continuous casting of steel, strand surface temperature profile and metallurgical length are two key processing variables that require real-time control to meet product quality and operational safety demands. The main focus of the control methods currently used in the steel industry is to maintain steel surface temperature. A common control method for secondary cooling is "spray table" or "speed-based" control, in which spray flowrates are interpolated from a look-up table, according to the current casting speed and the given spray pattern. The spray pattern defines the flowrates in each spray zone for each casting speed in the table, and depends on the steel grade, product dimensions and machine design.

Another widely used general class of control method is called "dynamic spray" control. These control methods include the concept of cooling time,[1] and are actually improved versions of spray table control. The original method has been called the residence time method, element lifetime method or effective lifetime method,[1] and is referred to as "time-constant" control in this paper. A more general dynamic spray cooling method, which combines the concepts of the spray table and cooling with time, is based on an empirical mixture constant, and is called the "effective speed" control method.[2,3] Effective speed control finds an effective casting speed (weighted speed of the average casting speed and the current casting speed) and uses it to calculate the spray flowrates from a given spray pattern. The concept is to deliver the same amount of water to each cross-section through the steel strand, according to the amount of time the slice has spent in the caster. Thus, these control methods smooth out the transient surface temperature fluctuations during sudden speed changes, relative to the sudden, detrimental temperature changes that occur with simple spray table control.[2]

However, for operations limited by the casting speed, or for steel grades that are more sensitive to centerline defects than to surface defects, the control of metallurgical length may be more important. Centerline segregation is a type of macrosegregation that appears as a line of impurities, and is accompanied by porosity, inclusions, alloy-rich regions and even cracks, distributed near the centerline along the slab length. These centerline defects are often very harmful, especially in highly alloyed steels, or when the slab is rolled into thin plates.[4]

Soft reduction technology has been developed to reduce centerline segregation. As shown in Fig. 1, during the solidification process, the steel shrinks the most while transitioning from liquid phase to solid phase. Therefore, the centerline is susceptible to segregation and other defects if the roll gap profile, which defines the taper of the entire casting machine, does not match the steel shrinkage. The choice of location of the soft reduction region depends on the shell thickness profile and the metallurgical length. If the steel is completely solid when the slab enters the soft reduction region, then the rolls experience large forces from the solid steel, which could damage both the slab and the rolls. If the steel is insufficiently solid upon entering the region, then soft reduction is insufficient where it is needed and centerline defects will arise. The soft reduction operation performs best

Figure 1

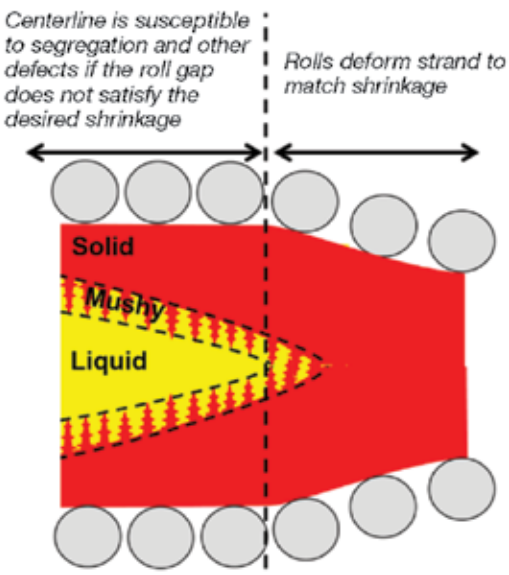

Soft reduction operation to reduce centerline segregation.

when the shell thickness profile and metallurgical length stay constant with time.

This paper explores the potential of using open-loop control for the task of maintaining metallurgical length during casting speed changes, by evaluating four different control methods for secondary cooling. A brief survey of these control methods is given. The dynamic model, CONOFFLINE (off-line version of the CONONLINE model[5]), has been calibrated with plant measurements and used to investigate the dynamic thermal behavior of a continuous steel slab caster during speed drops, under different secondary cooling control methods, and the metallurgical length variations are compared.

Control Methods Overview

The performance of the following four control methods on controlling the metallurgical length during speed drops are explored: (1) constant spray cooling (no control); (2) spray table control; (3) time-constant control; and (4) bang-bang control.

Constant Spray Cooling — The spray flowrates in the secondary cooling region are kept constant during speed changes. This lack of any control is used as a reference to compare the performance of other control methods.

Spray Table Control — For spray table control, the spray water flowrates in the different spray zones, or spray patterns, that produce good quality steel are determined by experience, plant trial and error, and steady-state modeling. Higher casting speed requires higher water flowrates to maintain the same cooling conditions. These spray patterns depend on steel grade, production dimension and machine design, and are tabulated as a function of casting speed. During the continuous casting process, if the casting speed changes, plant operators or an automatic level 2 control system will instantly change spray water flowrates by interpolating between the flowrates defined by the spray pattern for the casting speeds in the table above and below the actual casting speed.

Time-Constant Control — Under conditions of constant casting speed, the strand surface temperature at a given location z along the caster is constant and depends on the time it takes for the slice to reach that point from the meniscus, i.e., the "dwell time" of a slice, and the cooling conditions encountered. An increase in the casting speed will cause the dwell time to decrease, while the opposite will occur with a decrease in speed. The idea of time-constant control method is to change the flowrates according to the dwell time.

Consider the following general case: at wall clock time $t = 0$, the caster starts casting and the steel is casting at time-varying casting speed $v_c(t)$, where z is an arbitrary location along the caster. The dwell time $\tau(z,t)$ is defined as the time taken for the steel to travel from the meniscus to location z at time t, and it can be found by solving the inverse of the following equation:

$$z = \int_{t-\tau(z,t)}^{t} v_c(s)ds \qquad \text{(Eq. 1)}$$

Then, the average casting speed $\bar{v}_c$ for a slice to reach location z from the meniscus can be calculated by the following equation:

$$\bar{v}_c(z,t) = \frac{z}{\tau(z,t)} \qquad \text{(Eq. 2)}$$

In the continuous casting process, a spray zone typically can have just one spray flowrate over the entire zone, so instead of average casting speed for location z, $\bar{v}_c(z,t)$, the average casting speed is calculated for spray zone i at time t, $\bar{v}_i(t)$:

$$\bar{v}_i(t) = \frac{z_{mid}(i)}{\tau(z_{end}(i),t)} \qquad \text{(Eq. 3)}$$

where

$z_{mid}(i)$ and $z_{end}(i)$ = distance from the meniscus to the middle and end of spray zone i and
$\tau(z_{end}(i),t)$ = dwell time for the steel to travel from the meniscus to the end of spray zone i.

Then $\overline{v}_i(t)$ is used to lookup the spray flowrate for spray zone i from the spray table.

Bang-Bang Control — In control theory, the bang-bang optimal controller, also known as the hysteresis controller, is a controller that switches abruptly between two or more states.[6] In this paper, bang-bang control was applied to the following optimization problem: control secondary spray cooling water to minimize the metallurgical length fluctuation during casting speed change within the spray flowrate constraints of each spray zone. Three different types of bang-bang control were investigated here: single-step bang-bang, two-step bang-bang and three-step bang-bang control sequences. For single-step bang-bang control, the flowrates only switch once after the speed drop. At the optimal chosen time, t^i_{1b}, the flowrate at each spray zone switches from $Q^i_{sw}(orig)$ (the spray pattern before speed change) to $Q^i_{sw}(final)$ (the final spray pattern). Under single-step bang-bang control, the flowrate of spray zone i is calculated as follows:

$$Q^i_{sw\_1b} = \begin{cases} Q^i_{sw}(orig) \ if \ t < t^i_{1b} \\ Q^i_{sw}(final) \ if \ t \geq t^i_{1b} \end{cases} \quad \text{(Eq. 4)}$$

where

Q^i_{sw} = spray cooling water flowrate in spray zone i and
t^i_{1b} = switching time for spray zone i.

For two-step bang-bang control, the spray flowrate for each spray zone switches twice. After the speed drop, the flowrate first immediately switches to the minimum flowrate allowed, and then at a pre-determined switching time, the flowrate switches to the value from the calibrated spray pattern for the final casting speed, denoted as $Q^i_{sw}(final)$. Under two-step bang-bang control, the flowrate of the spray zone i is found from:

$$Q^i_{sw\_2b} = \begin{cases} Q^i_{sw}(orig) \ if \ t < t^i_{2b1} \\ Q^i_{sw}(min) \ if \ t^i_{2b1} < t < t^i_{2b2} \\ Q^i_{sw}(final) \ if \ t \geq t^i_{2b2} \end{cases} \quad \text{(Eq. 5)}$$

where

t^i_{2b} = two switching times for spray zone i and
$Q^i_{sw}(final)$ = final flowrate for spray zone i.

For three-step bang-bang control, the flowrate is found from:

$$Q^i_{sw\_3b} = \begin{cases} Q^i_{sw}(orig) \ if \ t < t^i_{3b1} \\ Q^i_{sw}(min) \ if \ t^i_{3b1} < t < t^i_{3b2} \\ Q^i_{sw}(3b) \ if \ t^i_{3b2} < t < t^i_{3b3} \\ Q^i_{sw}(final) \ if \ t \geq t^i_{3b3} \end{cases} \quad \text{(Eq. 6)}$$

where

t^i_{3b} = three switching times for spray zone i and
$Q^i_{sw}(3b)$ and $Q^i_{sw}(final)$ = switching water flowrate and final flowrate for spray zone i.

t^i_{3b} and $Q^i_{sw}(3b)$ can be controlled and need to be determined in advance. Under three-step bang-bang control, after the speed drop, the spray flowrate at spray zone i first drops to the minimum flowrate allowed $Q^i_{sw}(mm)$, then at time t^i_{3b2}, the flowrate switches to $Q^i_{sw}(3b)$; at time t^i_{3b3}, the flowrate switches to the final value $Q^i_{sw}(final)$.

In this work, the parameters t^i_b, t^i_{2b}, t^i_{3b}, $Q^i_{sw}(3b)$ for the above bang-bang control sequences were tuned based on the CONONLINE model prediction of the metallurgical length under corresponding bang-bang control sequences.

Model Description

A brief overview of the CONOFFLINE model, the off-line version of the CONONLINE model that was described in Reference 5, will be given in this section. The control diagram in Fig. 2 is realized in CONOFFLINE. CONOFFLINE uses recorded or specific casting conditions as inputs for the software sensor (Consensor), and different control methods are applied to this model. CONOFFLINE can be used to investigate the behavior of casters, especially phenomena such as transient evolution of the shell thickness profile, which cannot be easily measured.

Software Sensor — For a solidifying domain with heat transferred by internal conduction and advection, conservation of energy satisfies the following partial differential equation (PDE):

$$\rho c_p^* \left(\frac{\partial T}{\partial t} + \vec{v} \cdot \nabla T \right) = \nabla \cdot (k \nabla T) \quad \text{(Eq. 7)}$$

Figure 2

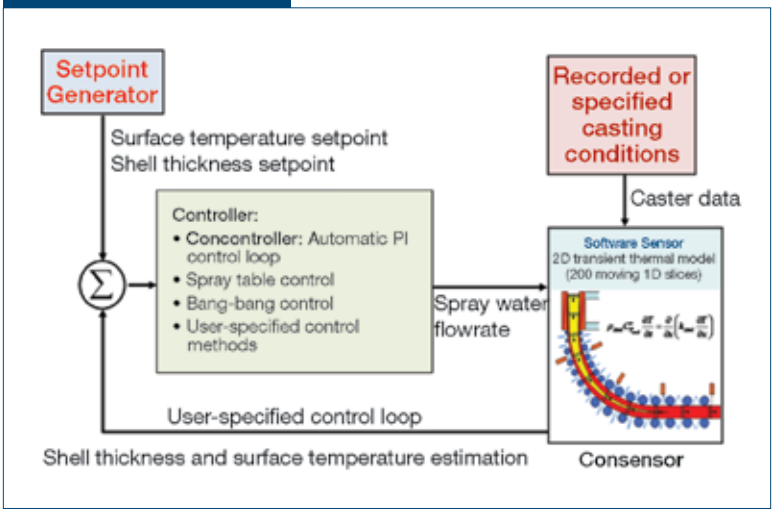

Control diagram of CONOFFLINE.

where

$T(x, y, z, t)$ = temperature at a given point (x, y, z) in the cast strand and
$\vec{v} = (v_x, v_y, v_z)$ is the velocity of the material at that point.

For this work, z denotes the casting direction, x denotes the thickness direction (narrow-face cross-sectional dimension) and y denotes the width direction (wide-face cross-sectional dimension). The origin of the x- and y-axes are at the center of the strand and the origin of z-axis is at the meniscus. The density ρ, the thermal conductivity k and the effective specific heat c_p^* are the properties of the cast material. The effective specific heat includes the latent heat:

$$c_p^* = c_p + L_f \frac{df_s}{dT} \quad \text{(Eq. 8)}$$

where

c_p = usual specific heat,
L_f = latent heat and
f_s = solid fraction of the steel.

The material in the steel strand moves in the z direction at casting speed v_c, and conduction in the y direction only matters near the corners of the slab. Furthermore, owing to the large Peclet number,[5] conduction is negligibly small compared to the advection in the z direction, and adopting a Lagrangian "slice" domain, which moves in the z-direction at the casting speed, Eq. 7 simplifies to:

$$\rho c_p^* \frac{\partial T}{\partial t} = \frac{\partial}{\partial x}\left(k \frac{\partial T}{\partial x}\right) \quad \text{(Eq. 9)}$$

Eq. 9 could be solved faster than real time, but it only gives the temperature estimation at the locations of the moving reference frame, which in return depends on the local casting speed history. By repeating the calculation for multiple slices simultaneously, CONSENSOR can produce the temperature profile along the entire caster (z) and through its thickness (x) in real time. It does this by managing the simulation of N different slices, each starting at the meniscus at different times to achieve a fixed z-direction spacing between the slices.

Currently, CONSENSOR manages exactly 200 slices, which corresponds to a uniform spatial interval of 0.255 m along the entire simulation domain for the illustrative example case based on the JFE Steel thick-slab caster, z_{total} = 51 m. After the first slice is created at the meniscus, whenever the most recent slice moves downward 0.255 m, a new slice is generated at the meniscus and starts moving downward. If an old slice moves out of containment, a new slice starts from the meniscus. By using this method, there are always 200 slices in the whole caster after start-up.

Model Validation — The CONONLINE model was recently validated by Petrus[7] for transient conditions. Specifically, the validation was done by comparing the simulation results of transient changes in the metallurgical length during casting speed changes with the plant measurements conducted on a 260-mm thick-slab caster at Burns Harbor during transient conditions.[8] During the trial, strain gauges were installed on some of the support rolls to measure the changing forces exerted on those rolls by the strand.

Fig. 9 in Reference 7 compares the prediction results from CONSENSOR and the measurements, showing good qualitative matches between the measured roll forces and the predicted thermal linear expansion (TLE) at the rolls. This figure shows the quantitative match between the timing of changes in roll force and the timing of changes in the thermal linear expansion predicted by CONSENSOR. Readers may refer to Reference 7 for more detailed information on validation of this model.

Table 1

Steel Properties in Simulation

Liquidus temperature	1,516.10°C
Solidus temperature	1,468.40°C
Peritectic temperature	1,486.50°C
Latent heat of solidification	271 kJ/kg

Table 2

Casting Conditions of the JFE Caster Simulations

Property	Value	Unit
Density of solid steel, ρ	7,400	kg/m^3
Steel emissivity, ε_{steel}	0.8	/
Solid fraction for shell thickness location, f_s	0.3	/
Specific heat of solid steel, c_p	670	J/kg · K
Thermal conductivity of solid steel, k	30	W/mK
Thermal diffusivity of solid steel, α	6.0508×10^{-6}	/
Initial cooling water temperature, T_{water}	29.67	°C
Slab thickness, L_x	221	mm
Slab width, L_y	2,095	mm
Ambient temperature, T_∞	35	°C
Pouring temperature, T_{pour}	1,545	°C
Time step	0.01	second
Mesh size	0.55	mm

Dynamic Simulation

Casting Conditions — The caster and casting conditions simulated in this work were based on the thick-slab (221 mm) caster at JFE Steel, Japan. The typical low-carbon steel grade studied in this work has the properties given in Table 1.

Based on an empirical correlation proposed by Duvvuri,[9] the average heat flux in the mold was set to:

$$Q_m\left[MW/m^2\right] = 1.2154\left(v_c\right)^{0.47} \quad \text{(Eq. 10)}$$

The coefficient and exponent were adjusted to match data from JFE Steel. More casting conditions are listed in Table 2. For the heat flux of the spray cooling water in the secondary cooling region, Nozaki's empirical correlation[10] was used:

$$h_{spray} = 0.3925 \times Q_{water}^{0.55} \times \left(1 - 0.0075 \times T_{spray}\right) \quad \text{(Eq. 11)}$$

where

Q_{water} (L/m^2) = water flux and
T_{spray} = temperature of the cooling water spray.

The heat transfer in the secondary cooling region is a subject of ongoing research, and other relations are available and used at different casters (including JFE).

Table 3

Spray Flowrate Limitations of Each Spray Zone

Zone	Q^i_{sw}(max) (L/minute/row)	Q^i_{sw}(min) (L/minute/row)
1	250.0	75.0
2	286.7	28.7
3	360.0	36.0
4	200.0	10.0
5	200.0	10.0
6	90.0	4.5
7	90.0	4.5
8	60.0	3.0
9	30.6	1.53
10	15.0	1.0
11	15.0	1.0
12	15.0	1.0

Table 4

Spray Patterns That Give Same Metallurgical Length

Zone	1.7_orig (L/minute/row)	1.5_sameML (L/minute/row)
1	90.2	75.0
2	61.9	55.0
3	98.2	56.6
4	127.9	40.0
5	111	30.0
6	70.9	20.0
7	51.0	14.4
8	19.1	5.0
9	6.0	3.9
10	4.1	3.4
11	3.6	2.8
12	6.5	5.6

Figure 3

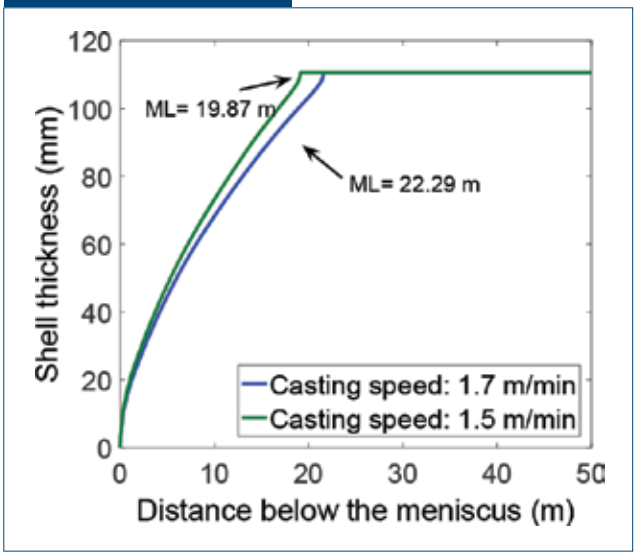

Shell thickness at steady state.

Figure 4

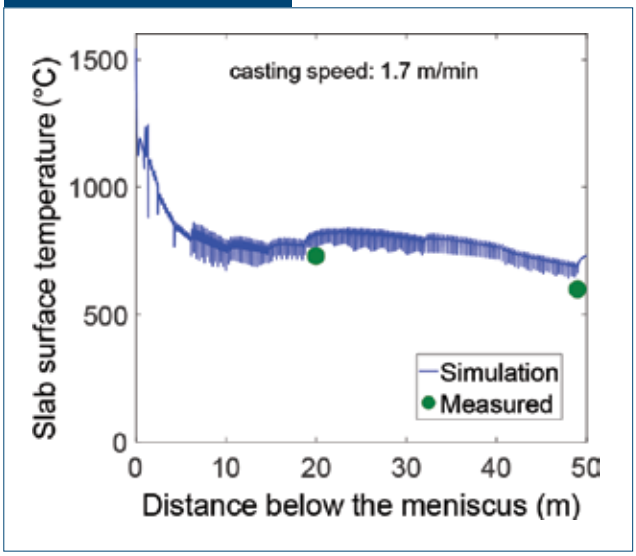

Surface temperature at steady state of 1.7 m/minute.

The speed change scenario simulated in this work is a sudden speed drop from 1.7 to 1.5 m/minute. However, in the real caster, there are limits of sudden speed drops that can be applied during the continuous casting process. If a sudden speed drop is too large, the flow control system may be unable to maintain constant steel flow into the caster and cause problems such as severe level fluctuations and breakouts, especially for thick-slab casters. Therefore, when a large speed drop is needed during operation, the speed drop is made in several steps, or made gradually over a time interval (usually several seconds).

The speed drop of 0.2 m/minute studied in this work is small. The results of steady-state simulation show that under this small speed drop, the same metallurgical length is achievable at these two casting speeds by applying feasible water flowrates. The limitations of spray flowrates for each spray zone, i.e., the maximum and minimum flowrates allowed, are listed in Table 3. At each spray zone, there is a series of rows of spray nozzles; the spray flowrates of spray zone i, denoted as Q^i_{sw} (L/minute/row) throughout this work, is the water flowrate for each row of spray nozzles in spray zone i.

In order to investigate the dynamic thermal behavior of the steel strand during changes between two specific speeds (1.5 m/minute and 1.7 m/minute), the original spray table was modified to make a hypothetical, but still realistic, example of part of a spray table, given in Table 4. Specifically, the water flowrates used when casting at 1.5 m/minute were dropped to spray pattern "1.5_sameML" in order to match the metallurgical length when casting at 1.7 m/minute, with the spray pattern "1.7_orig," based on steady-state simulations using the same mold heat flux Eq. 10 and the Nozaki equation.

For the secondary cooling region, three different control methods were applied to explore their performance on maintaining the metallurgical length: constant spray cooling, spray table control and bang-bang control. Before running simulations of different control methods, CONOFFLINE model was first calibrated according to the provided casting conditions. Fig. 3 shows the shell thickness profiles at steady state for two casting speeds, using standard spray table cooling patterns that produce similar surface temperature profiles. The predicted metallurgical lengths of both speeds match the measured data. Fig. 4 shows that the predicted surface temperatures agree with the measurements at steady state as well. After this calibration, the CONONLINE model was ready for further simulations.

Fig. 5 shows the model predictions of the surface temperature histories and the shell thickness profiles under the two different spray patterns, 1.7_orig and 1.5_sameML. The shell thickness profile with spray pattern 1.5_sameML cast at 1.5 m/minute is almost identical to that with spray pattern 1.7_orig at 1.7 m/minute. Therefore, the metallurgical lengths are the same as well. Fig. 5 also indicates a large temperature difference between two steady-state temperature profiles, which is expected. Because it is not possible to maintain both surface temperature and metallurgical length to be constant during a speed change, severe changes of the surface temperature during the speed changes are not the main concern of this study.

The results in Fig. 5 show that under the small speed drop of 0.2 m/minute studied here, constant

Figure 5

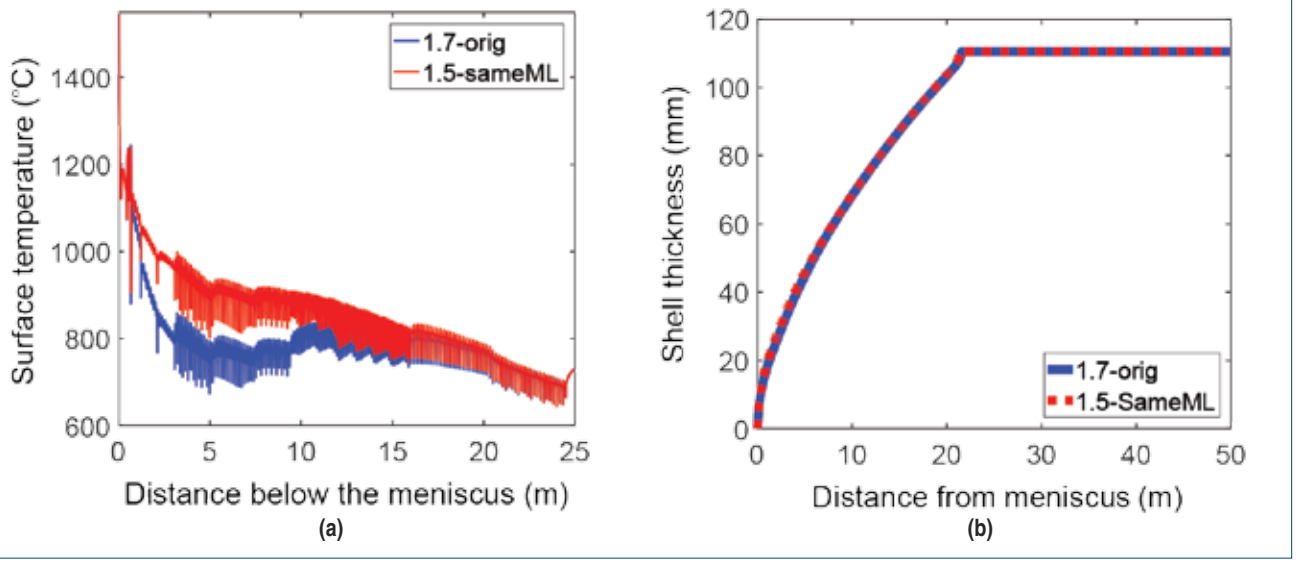

CON1D model prediction of surface temperature and shell thickness profile under different spray patterns.

metallurgical lengths at both casting speeds are achievable by applying the largest feasible water flowrates possible under steady-state conditions for this caster. The metallurgical length deviation, defined as the difference (undershoot and/or overshoot) between the metallurgical length at 1.7 m/minute and the final metallurgical length after the speed drop, is used to compare their performance. For all of the simulations below, the speed change is assumed to happen at $t = 0$.

Constant Spray Cooling (No Spray Control) — In order to compare the performance of different control methods, the "no control" case was simulated first, keeping the spray flowrates everywhere in the secondary cooling region constant throughout the speed drop. The specific spray flowrates used are the values from the spray pattern of 1.7_orig. The model prediction of the metallurgical length after the speed drop is shown in Fig. 6. After the speed drop, the metallurgical length decreases linearly. By 776 seconds after the speed drop, the steel is fully solid around 19.57 m and the maximum metallurgical length deviation is a decrease of 2.72 m.

Figure 6

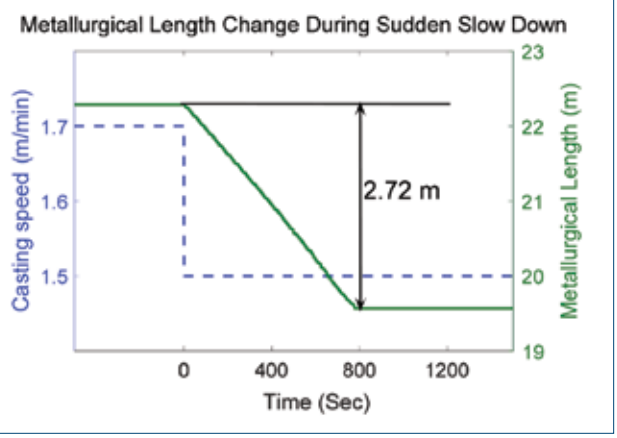

Model prediction of metallurgical length (ML) changes during the speed drop under constant spray cooling.

Figure 7

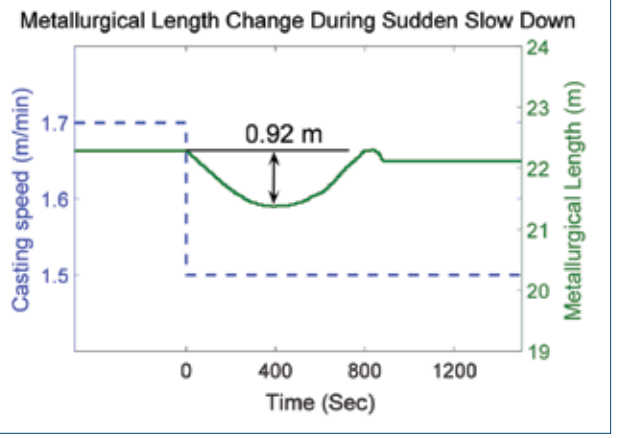

Model prediction of ML under spray table control.

Figure 8

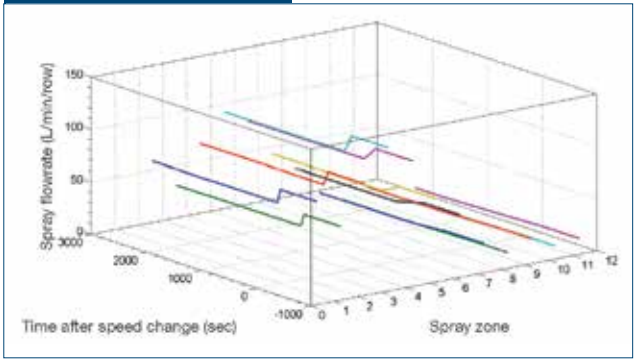

Flowrates under spray table control.

Figure 9

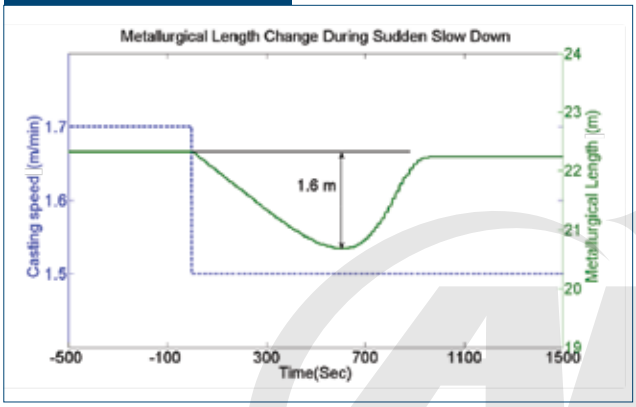

Model prediction of ML under spray table control.

Spray Table Control — Applying spray table control to the secondary cooling region using the spray patterns given in Table 4 gives the following water flowrates equation:

$$Q^i_{sw}(t) = Q^i_{sw}(v_c(t)) = Q^i_{sw}(1.5\_sameML)\frac{1.7 - v_c}{0.2} + Q^i_{sw}(1.7\_orig)\frac{v_c - 1.5}{0.2}$$

(Eq. 12)

Fig. 7 indicates that after the speed drop, the metallurgical length gradually decreases, then increases, and finally reaches steady state after a small overshoot. The metallurgical lengths before and after the speed drop under steady state are almost the same; the deviation of the metallurgical length for spray table control under the spray patterns of 1.7_orig and 1.5_sameML is an undershoot of 0.92 m followed by an overshoot of 0.18 m. The metallurgical length deviation is reduced by 66.1% compared with the constant spray cooling case. The overshoot would be a potential concern for whale formation, if the metallurgical length was near the end of containment. However, this overshoot is small, within the deviation remaining at steady-state for this set of conditions.

Time-Constant Control — The average casting speed history for each zone $\bar{v}_i(t)$ can be calculated by Eq. 3; which is then used to calculate the spray flowrate changes with time based on the spray patterns 1.7_orig and 1.5_sameML by replacing v_c in Eq. 12 with $\bar{v}_i(t)$.

Fig. 8 shows the spray flowrate histories calculated during the speed drop. Fig. 9 shows the metallurgical length profile under the time-constant control method; the deviation of the metallurgical length is an undershoot of 1.6 m with no overshoot. Compared with the constant spray cooling case, the metallurgical length deviation is reduced by 41.2%. Compared with Fig. 7, the metallurgical length deviation under time-constant control is larger than that under spray table control. This is because the flowrates change gradually during transition under the time-constant method, the steel receives more water; thus, more heat is extracted by spray cooling water, which leads to smaller minimum metallurgical length and larger metallurgical length deviation.

Bang-Bang Control

Single-Step Bang-Bang Control: To implement single-step bang-bang control as a real control method, the metallurgical lengths before and after the speed change should be the same, so the water flowrate of spray zone i is calculated by:

$$Q^i_{sw\_1b} = \begin{cases} Q^i_{sw}(1.7\_orig) \text{ if } t < t^i_{1b} \\ Q^i_{sw}(1.5\_sameML) \text{ if } t \geq t^i_{1b} \end{cases}$$

(Eq. 13)

To achieve minimum metallurgical fluctuation, the flowrates at each zone need to drop immediately after speed drop, i.e., $t^i_{1b} = 0$, then this method is identical to spray table control.

For both two-step and three-step bang-bang control sequences, the first switch is the same, i.e., after the speed drop, the flowrates immediately drop to the minimum flowrates allowed for all spray zones to minimize the heat removal and shell growth. It is vital to study the effect of the first switch, because it affects the selection of the parameters for these other two control sequences.

In this section, the first switch of the other two bang-bang control sequences is studied. The flowrates for different spray zones under single-step bang-bang control are described in Eq. 4, with $t^i_{1b} = 0$ for all spray zone i. Fig. 10 shows the CONOFFLINE model

Figure 10

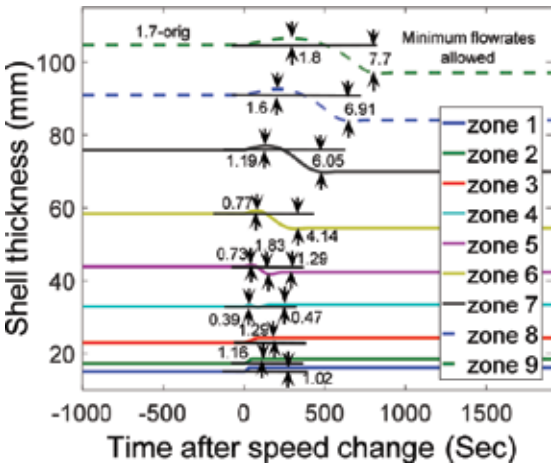

Model prediction of average shell thickness of all spray zones under single-step bang-bang control.

Figure 11

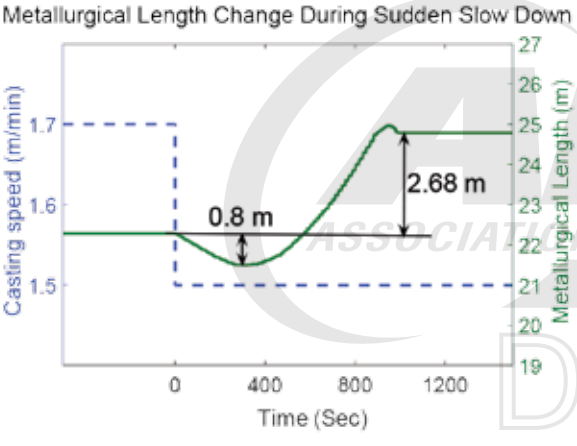

Model prediction of metallurgical length under single-step bang-bang control.

Table 5

Switching Time of the Two-Step Bang-Bang Control Sequence

Zone (i)	t^i_{2b1}(sec)	t^i_{2b2}(sec)
4	0	30
5	0	48
6	0	80
7	0	140
8	0	180
9	0	296

prediction of the average shell thickness in zones 1–9 for single-step bang-bang control; zones 10–12 are neglected because the steel strand is already fully solid before entering zone 10. Fig. 11 shows the metallurgical length profile under single-step bang-bang control: the metallurgical length has the opposite transient behavior as the behavior of the average shell thickness shown in Fig. 10. Fig. 11 indicates two important findings: (1) the minimum undershoot of the metallurgical length possible is 0.8 m; (2) to keep metallurgical lengths under steady state the same, two-step bang-bang control with a second switch to be the flowrates in spray pattern 1.5_sameML should be applied.

Two-Step Bang-Bang Control: In order to match the metallurgical lengths at steady state for the two casting speeds, the second step (final) flowrates are chosen to be the flowrates from the spray pattern 1.5_sameML. Therefore, from Eq. 5, the remaining parameters that need to be chosen are the switching times t^i_{2b} for all spray zones. These switching times can vary for different spray zones.

The metallurgical length is determined by the shell thickness profile of the spray zone in which the steel strand becomes fully solid, i.e., zone 9 in this case. However, the shell thickness behavior in the upper zones will affect the behavior in zone 9. Therefore, the switching times of the second switch t^i_{2b} were tuned sequentially and separately for every spray zone based on the average shell thickness profile of the corresponding zone. Eq. 5 then becomes the following:

$$\text{for } i\text{=4-9: } Q^i_{sw\_2b}(t) = \begin{cases} Q^i_{sw}(1.7\_orig) & \text{if } t < t^i_{2b1} \\ Q^i_{sw}(min) & \text{if } 0 \le t \le t^i_{2b2} \\ Q^i_{sw}(1.5\_sameML) & \text{if } t \ge t^i_{2b2} \end{cases}$$

$$\text{for } i\text{=1-3,10-12: } Q^i_{sw\_2b}(t) = Q^i_{sw\_1b}(t)$$

(Eq. 14)

where the switching times for zones 4–9 are shown in Table 5. For the other zones, the spray flowrates are the same as $Q^i_{sw\_1b}$ with $t^i_{1b} = 0$, i.e., the same as spray table control.

The flowrates under the two-step bang-bang control sequence are shown in Fig. 12. The model prediction of the metallurgical length history is shown in Fig. 13, with a maximum metallurgical length deviation of 0.8 m. Compared with the constant spray cooling case, the metallurgical length deviation is reduced by 70.6%. However, there is a small overshoot (0.37 m) before reaching steady state, which is unable to be removed with two-step bang-bang control sequence while still maintaining the 0.8 m maximum metallurgical length deviation. The reason is that, to remove the overshoot, more cooling water

Figure 12

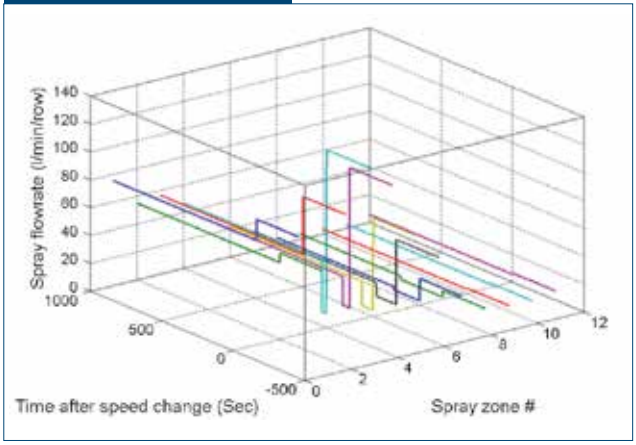

Flowrates of two-step bang-bang control.

Figure 13

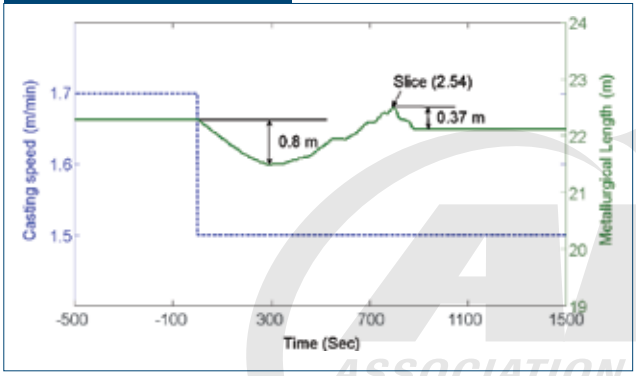

Model prediction of ML under two-step bang-bang control.

Figure 14

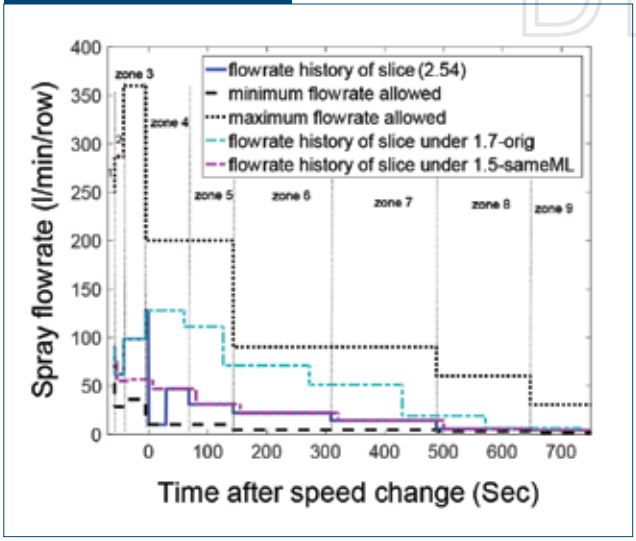

Flowrate history for slice (2.54) shown in Fig. 13.

must be added to the slice, which has the maximum metallurgical length, i.e., slice (2.54) (which is 2.54 m away from the meniscus when the speed drop happens). Fig. 14 shows the flowrate history of slice (2.54); the results show that the flowrates in zones 5–9 have already reached the values from the spray pattern of 1.5_sameML when slice (2.54) enters the spray zones. If more cooling water is needed for slice (2.54), the flowrate in zone 4 needs to be increased, i.e., decrease t^A_{2b2}, but this might increase the metallurgical length deviation per the previous discussion.

To better straighten out the response (decrease the overshoot), three-step bang-bang control is considered: a full step down, a bit earlier strong step up and then a small step down.

Three-Step Bang-Bang Control: To reduce the overshoot shown in the metallurgical length profile in Fig. 13, another bang-bang control sequence, which added a third sudden step (switch) to the two-step bang-bang control sequence, is applied to the model. In three-step bang-bang control, there are three sets of parameters to be determined: t^i_{3b2}, t^i_{3b3}, $Q^i_{sw}(3b)$. The first switch is assumed to occur at the time of speed drop, t^1_b, in all cases.

From the discussion in the previous section, to reduce the overshoot, the amount of spray cooling water received by slice (2.54) in spray zone 4 needs to be increased. Therefore, three-step bang-bang control is first only applied in zone 4, and two-step bang-bang control sequence is applied in the rest of

Figure 15

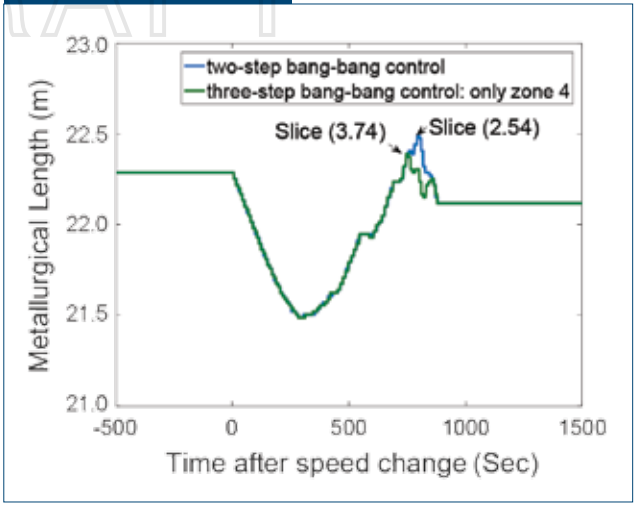

Comparison of ML for two-step bang-bang control sequence and three-step bang-bang control sequence only applied in zone 4.

Table 6

Parameters of Three-Step Bang-Bang Controller

Zone (i)	t^i_{3b1}(sec)	t^i_{3b2}(sec)	t^i_{3b3}(sec)	Q^i_{sw}(3b) (L/min/row)
4	0	30	60	98.2
5	0	48	110	55
6	0	80	130	30
7	0	110	140	20

the zones. $Q^4_{sw}(3b)$ is chosen to be 98.2 L/minute/row, and t^4_{3b}, t^4_{3b2} are chosen to be 30 seconds and 60 seconds. This set of parameters give roughly the same amount of cooling water for slice (2.54) in zone 4 as in 1.5_sameML. The metallurgical length transient behavior of the above case is shown in Fig. 15. The result shows that the slice that has the maximum metallurgical length is now slice (3.74). The metallurgical length for slice (2.54) and the slices near it were reduced. Although the spray flowrate in the spray zone 4 was tuned specially for slice (2.54), the spray flowrate in the whole zone is changed and affected the other slices in zone 4. Now repeat the same method for slice (3.74). By this tuning method, the set of parameters listed in Table 6 is finally chosen.

Note that three-step bang-bang control was only applied to zones 4–7. For the other zones, the spray flowrates are the same as two-step bang-bang control. Eq. 6 is then modified to the following:

$$for\ i=4\text{-}7:\ Q^i_{sw\_3b}(t)=\begin{cases} Q^i_{sw}(1.7\_orig) & if\ t<t^i_{3b1} \\ Q^i_{sw}(min) & if\ 0\le t\le t^i_{3b2} \\ Q^i_{sw}(3b) & if\ t^i_{3b2}\le t\le t^i_{3b3} \\ Q^i_{sw}(1.5\_sameML) & if\ t\ge t^i_{3b3} \end{cases}$$

$$for\ i=1\text{-}3,8\text{-}12:\ Q^i_{sw\_3b}(t)=Q^i_{sw\_2b}(t)$$

(Eq. 15)

The flowrate histories of all spray zones are shown in Fig. 16. The result of the metallurgical length profile under three-step bang-bang control sequence is shown in Fig. 17. Same as the two-step bang-bang control sequence, the maximum deviation of metallurgical length is 0.8 m. Compared with the constant spray cooling case, the metallurgical length deviation is reduced by 70.6%. There is still a small overshoot (0.1 m) in the metallurgical length profile, but slice (0.8), which has a maximum metallurgical length in the overshoot region, is still in the mold when the speed change happens. When it enters each spray zone, the spray flowrates are already in steady state of 1.5_sameML, which means the overshoot is not caused by the secondary cooling but the primary cooling.

Discussion

For the objective of controlling metallurgical length, it is only feasible to achieve constant metallurgical length for a small speed drop of 0.2 mm/minute from 1.7 to 1.5 m/minute for a typical thick slab caster. Spray table control based on spray patterns of 1.7_orig and 1.5_sameML are close to the maximum and minimum flowrates, and thus produce a significant increase in surface temperature for the lower speed. This reduces the maximum deviation of the metallurgical length by 66.1%, decreasing the undershoot from 2.72 m (with no control) to 0.92 m.

The time-constant control method based on the same spray patterns reduces the maximum deviation of metallurgical length by only 41.2%. Thus, time-constant control is not as good at controlling metallurgical length, although it is much better than spray table control at maintaining surface temperature during the speed change.

Two-step and three-step bang-bang control sequences produce maximum metallurgical length dips of 0.8 m, reducing the metallurgical length undershoot

Figure 16

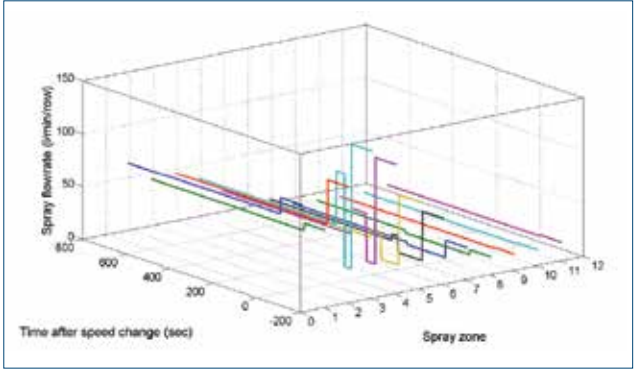

Flowrates of three-step bang-bang control.

Figure 17

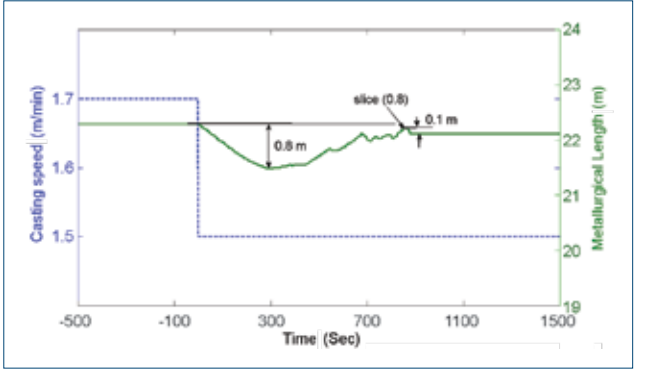

Model prediction of ML under three-step bang-bang control.

by 70.6%. Thus, the bang-bang control sequences have better performance at maintaining the metallurgical length. Moreover, three-step bang-bang control has much smaller overshoot of the metallurgical length profile. Overall, the three-step bang-bang control sequence has the best performance at controlling the metallurgical length during the speed drop among all the methods studied. However, this method causes sudden changes in the surface temperature profile, which are very likely to cause cracks. So, this method is likely not the most optimal control method overall.

Conclusions

In this paper, the behavior of the metallurgical length during a sudden drop in casting speed was investigated with four control methods. Simulation results demonstrate that the controllability of the metallurgical length is limited even for a small speed drop of 0.2 m/minute. Bang-bang control has the best performance with minimum metallurgical length deviation of 0.8 m. Sudden speed change is not recommended. Further work is needed to evaluate control methodologies for different control objectives together.

Acknowledgments

This work was supported by NSF Grant #CMMI-1300907 and the Continuous Casting Consortium at the University of Illinois at Urbana-Champaign. Special thanks are given to JFE Steel Corp. for providing caster data and casting conditions.

References

1. J. Brimacombe, P. Agarwal, S. Hibbins, B. Prabhaker and L. Baptista, *Spray Cooling in the Continuous Casting of Steel,* ISS/AIME, 1984, pp. 109–123.
2. Z. Dou, Q. Liu, B. Wang, X. Zhang, J. Zhang and Z. Hu, "Evolution of Control Models for Secondary Cooling in Continuous Casting Process of Steel," *Steel Research International,* Vol. 82, No. 10, 2011, pp. 1220–1227.
3. L. Klimes and J. Stetina, "Challenges in Numerical Modeling of Continuous Steel Casting — Very Fast GPU Dynamic Solidification Model and Its Use in Continuous Casting Control," *European Continuous Casting Conference,* 2014.
4. J. Sirgo, R. Campo, A. Lopez, A. Diaz and L. Sancho, "Measurement of Centerline Segregation in Steel Slabs," *IEEE Industry Applications Conference,* 2006.
5. B. Petrus, K. Zheng, X. Zhou, B.G. Thomas and J. Bentsman, "Real-Time Model-Based Spray-Cooling Control System for Steel Continuous Casting," *Metallurgical and Materials Transactions B,* Vol. 42, No. 1, 2011, pp. 87–103.
6. D. Liberzon, *Calculus of Variations and Optimal Control Theory: A Concise Introduction,* Princeton University Press, 2011.
7. B. Petrus, D. Hammon, M. Miller, B. Williams, A. Zewe, Z. Chen, J. Bentsman and B.G. Thomas, "New Method to Measure Metallurgical Length and Application to Improve Computational Models," *Iron & Steel Technology,* Vol. 12, No. 12, 2015, pp. 58–66.
8. N. Gregurich, G. Flick, R. Moravec and K. Blazek, "In-Depth Analysis of Continuous Caster Machine Behavior During Casting With Different Roll Gap Taper Profiles," *Iron & Steel Technology,* Vol. 9, No. 12, 2012, p. 62.
9. P. Duvvuri, B. Petrus and B.G. Thomas, "Correlation for Mold Heat Flux Measured in a Thin-Slab Casting Mold," *AISTech 2014 Conference Proceedings,* Vol. III, 2014, pp. 2881–2893.
10. T. Nozaki, J. Matsuno, K. Murata, H. Ooi and M. Kodama, "A Secondary Cooling Pattern for Preventing Surface Cracks of Continuous Casting Slab," *Transactions of the Iron and Steel Institute of Japan,* Vol. 18, No. 6, 1978, pp. 330–338. ✦

AISTech This paper was presented at AISTech 2017 — The Iron & Steel Technology Conference and Exposition, Nashville, Tenn., USA, and published in the Conference Proceedings.

Did You Know?

Industry 4.0: A Made-in-Italy Project for Metal 3D Printing

A "widespread" factory for the development of metal 3D printing technology: this is the objective of the project Metal AdditivE for LOmbardy (MADE4LO), which will start this autumn under the leadership of Tenova. The goal of the project is to cover the entire value chain, creating a new model of factory based on 3D manufacturing, network infrastructure, digital processes and intensive training.

The project, partially funded by the European Regional Development Fund, will last 30 months for a total investment of 6.6 million euros, involving 11 partners from Lombardy, Italy: two universities (Politecnico di Milano and Università di Pavia), three big industries (Tenova, BLM and GF Machining Solutions), and six small and medium-sized enterprises (TTM Laser, 3D-NT, GFM, Fubri, Co. Stamp and Officine Meccaniche G. Lafranconi).

Metal additive manufacturing (AM), also known as metal 3D printing, allows for production of complex three-dimensional objects from a 3D CAD model by adding material layer by layer, without the constraints of traditional manufacturing routes. AM is emerging as a competitive process for the production of series components for demanding applications while reducing material inventory.

All of Tenova Metals' business units are involved in MADE4LO to define the most cost-effective equipment to select, design and test the metal components to produce by AM, and to design and manufacture a heat treatment furnace to be installed at its Pomini factory.

"MADE4LO is the first pilot project developed in Lombardy in the field of additive manufacturing which involves a network of physical and digital systems interconnected with each other, which exchange products and information through a widespread infrastructure (digital information on the product to be printed, powder and process data, data gathered from the process related to the qualification of the realized products)," commented Prof. Marco Bocciolone, director of the Mechanics Department of Politecnico di Milano.

Prof. Barbara Previtali, scientific supervisor of the project, pointed out how the focus of applications and the sectors of development targeted through MADE4LO go beyond the area where additive processes are currently applied. "MADE4LO will explore new applications in relevant sectors like the printing of new metals' components (such as copper and tool steel alloys) or the additive and subtractive repairing/revamping of big components of high added value."